The American Journal of Pathology, Vol. 173, No. 4, October 2008

DOI: 10.2353/ajpath.2008.071062

Growth Factors, Cytokines, Cell Cycle Molecules

Absence of the Cellular Prion Protein Exacerbates and Prolongs Neuroinflammation in Experimental Autoimmune Encephalomyelitis

Shigeki Tsutsui, Jennifer N. Hahn, Trina A. Johnson, Zenobia Ali, and Frank R. Jirik

From the Department of Biochemistry and Molecular Biology, McCaig Institute for Bone and Joint Health, University of Calgary, Calgary, Alberta, Canada

Although the physiological roles of the cellular prion protein (PrP^C) remain to be fully elucidated, PrP^C has been proposed to represent a potential regulator of cellular immunity. To test this hypothesis, we evaluated the consequences of PrP^C deficiency on the course of experimental autoimmune encephalomyelitis induced by immunization with myelin oligodendrocyte glycoprotein peptide. Consistent with augmented proliferative responses and increased cytokine gene expression by myelin oligodendrocyte glycoprotein-primed *Prnp*$^{-/-}$ T cells, PrP^C-deficient mice demonstrated more aggressive disease onset and a lack of clinical improvement during the chronic phase of experimental autoimmune encephalomyelitis. Acutely, *Prnp*$^{-/-}$ spinal cord, cerebellum, and forebrain exhibited higher levels of leukocytic infiltrates and pro-inflammatory cytokine gene expression, as well as increased spinal cord myelin basic protein and axonal loss. During the chronic phase, a remarkable persistence of leukocytic infiltrates was present in the forebrain and cerebellum, accompanied by an increase in interferon-γ and interleukin-17 transcripts. Attenuation of T cell-dependent neuroinflammation thus represents a potential novel function of PrP^C. ***(Am J Pathol 2008, 173:1029–1041; DOI: 10.2353/ajpath.2008.071062)***

The cellular prion protein (PrP^C), a highly conserved glycosylphosphatidylinositol-anchored cell surface glycoprotein concentrated in lipid rafts,[1] is abundantly expressed in the central nervous system (CNS).[2,3] PrP^C may serve as a receptor for a variety of putative ligands, including: heparan sulfate,[4] laminin,[5] neural cell adhesion molecule,[6] various synaptic proteins,[7] and stress-inducible protein-1.[8] These ligand-receptor interactions suggest that PrP^C could have a role in diverse processes, including neurodevelopment, synaptic function, neurite outgrowth, and neuronal survival. Evidence for the latter has supported the notion that neuroprotection is one physiological function of PrP^C. For example, deletion of PrP^C increased neuronal predisposition to damage by modulating susceptibility to apoptosis[9,10] and the negative consequences of oxidative stress.[11–13] Furthermore, *in vivo* studies demonstrated that PrP^C-deficient mice were more prone to seizure induction,[14] and exhibited an increased extent of cerebral damage following an ischemic challenge.[15] In contrast, adenovirus-mediated PrP^C overexpression reduced CNS damage in a rat model of cerebral ischemia.[16] While the mechanism(s) underlying these phenomena remain unclear, such *in vivo* findings have lent strong support to the idea that PrP^C may have a neuroprotective function.

PrP^C is expressed on the surface of cells of the human and murine lympho-hematopoietic system, including dendritic cells (DCs), follicular dendritic cells, macrophages/microglia, and in humans, T-lymphocytes.[17–20] With regard to the latter, in mice PrP^C was only detected in a relatively small subset of mature B and T lymphocytes.[21,22] Recent studies have concluded that PrP^C may play a role in T cell activation,[23] the phagocytic ability of macrophages,[24] and T cell-DC interactions.[25] The interaction between T cells and DCs represents a critical event for the initiation of primary immune responses, and hence the finding that both T cells and DCs express PrP^C, raised the possibility that PrP^C plays a role in immune system homeostasis. Precisely how PrP^C

Supported by the Canadian Networks of Centres of Excellence Program (Genetic Diseases Network) and by the Alberta Agricultural Research Institute. Also, S.T. held a Fellowship from the Multiple Sclerosis Society of Canada, and F.R.J. was the recipient of a Canada Research Chair Award.

Accepted for publication June 26, 2008.

Supplemental material for this article can be found on http://ajp.amjpathd.org.

Address reprint requests to Frank R. Jirik, M.D., FRCPC, University of Calgary, 3330 Hospital Drive NW, Calgary, Alberta, Canada T2N 4N1. E-mail: jirik@ucalgary.ca.

might regulate the *in vivo* activities of cells of the immune system during normal or autoimmune T cell-mediated responses, however, remains nebulous.

Since PrP^C is expressed in cells of the murine immune system, we hypothesized that mice lacking this molecule might show an alteration in their response to an induced T cell-mediated autoimmune disease. We report that mice lacking PrP^C develop earlier onset, more severe EAE, and also that they fail to recover during the chronic phase of EAE. This novel phenotype was accompanied by histopathological evidence of greater involvement of cerebellum and forebrain, more extensive spinal cord damage, as well as a striking persistence of monocytic and T cell infiltrates in the CNS. PrP^C thus appears to be an important regulator of T cell-mediated neuroinflammation.

Materials and Methods

Induction of EAE

Mice with a targeted disruption of the prion gene *(Prnp)* of the Zurich I strain[26] and their controls (of a mixed 129 and Friend Leukemia virus B background) were obtained from the European Mouse Mutant Archive (EM:0158, EMMA-Rome Italy) and interbred to generate $Prnp^{-/-}$ and $Prnp^{+/+}$ littermates used in the experiments. The Zurich I mice, backcrossed for multiple generations (N = 7 to 8) into a C57BL/6 genetic background, were also used in some of the experiments. To induce EAE, 11 to 14 week-old females were injected subcutaneously at the base of the tail with 50 μg of myelin oligodendrocyte glycoprotein (MOG_{35-55})[27] emulsified in complete Freund's adjuvant CFA (Difco Laboratories, Sparks, MD), together with 300 ng of reconstituted lyophilized pertussis toxin (List Biological Laboratories, Campbell, CA) administered intraperitonealy. Pertussis toxin injection was repeated after 48 hours.[28] Animals were assessed for EAE clinical severity for 60 days ($Prnp^{+/+}$ and $Prnp^{-/-}$ animals) using a 0 to 5 rating scale[28] as follows: 0 = no disease; 1 = limp tail; 2 = partial paralysis of one or two hind limbs; 3 = complete paralysis of hind limbs; 4 = hind limb paralysis and fore limb paraparesis; and 5 = moribund. Mice were euthanized by cardiac puncture while under methoxyfluorane anesthesia at 60 days post-EAE induction. Animals were maintained in accordance with Canadian Council on Animal Care and University of Calgary Animal Care Committee regulations.

Dendritic Cell, Total T Cell, and $CD4^+$ T Cell Isolation and Fluorescence-Activated Cell Sorting Analysis

Spleens were obtained from non-immunized C57BL/6 $Prnp^{+/+}$ and $Prnp^{-/-}$ animals. DC-enriched populations and $CD4^+$ T cells were then isolated from dissociated splenocytes by negative selection using two magnetic separation systems: StemSep mouse dendritic cell enrichment kit and EasySep mouse $CD4^+$ T cell enrichment kit, in accordance with the manufacturer's instructions (StemCell Technologies Inc., Vancouver, BC, Canada). $CD4^+$ T cells were cultured in serum-free AIM V media containing 3% IL-2 conditioned media and 2 μmol/L β-mercaptoethanol; cells were stimulated with 1 μg/ml anti-CD3 antibody for 48 hours. For flow cytometric analysis, 1×10^6 cells/ml of either DCs or $CD4^+$ T cells were resuspended in 1% fetal bovine serum in PBS and incubated with anti-mouse CD16/32 (24G2, FcR block, BD Biosciences PharMingen, San Diego, CA) to prevent nonspecific staining. Cells were incubated with 5 μg/ml of anti-mouse PrP^C antibody (SAF-83, Cayman Chemical Company, Ann Arbor, MI) or mouse IgG_1 isotype control (BD Biosciences, San Jose, CA), and then incubated with 5 μg/ml of fluorescein isothiocyanate-conjugated goat anti-mouse Ig (BD Biosciences). Live cells were collected and gated using a FACSCalibur with CellQuest software (BD Biosciences) and quantified using FlowJo software (version 3.6; TreeStar, Ashland, OR).

T Cell Proliferation Assay

DC-enriched cells isolated from non-immunized C57BL/6 $Prnp^{+/+}$ and $Prnp^{-/-}$ mice were irradiated, suspended at a density of 1×10^6 cells/ml, and pulsed with 40 μg/ml MOG_{35-55} peptide for 30 minutes. DC-enriched cells incubated with vehicle served as the 'No MOG' controls. Draining lymph nodes were removed from MOG peptide-immunized (using the same protocol as for EAE induction described above) C57BL/6 $Prnp^{+/+}$ and $Prnp^{-/-}$ animals at 10 days post-immunization (dpi). Lymph nodes were homogenized in Roswell Park Memorial Institute (RPMI) 1640 media and total T cells were isolated from dissociated lymph nodes, using the EasySep mouse T cell enrichment kit, and suspended at a density of 2.5×10^6 cells/ml. DCs and T cells were plated 1:1 in 96-well U-bottom microtiter plates containing enriched RPMI 1640 media [RPMI 1640, 10% fetal calf serum, 1% L-glutamine, 1% minimum essential medium-nonessential amino acids, 2 μmol/L β- mercaptoethanol, 1% penicillin-streptomycin, and 1% sodium pyruvate]. Cells were then incubated at 37°C for 48 hours before adding 1 μCi [^{3}H] thymidine (MP Biomedicals Inc., Irvine, CA) to each well. Cells were harvested 24 hours later and counted on a liquid scintillation counter (LS3801, Beckman Instruments, Fullerton, CA).

Histological Analysis

Brains and spinal cords were removed from euthanized animals, immersed in 10% neutral buffered formalin and embedded in paraffin wax as described previously.[27] Sections (4 μm) taken from cervical and lumbosacral spinal cords were stained by Bielschowsky's silver impregnation method. Axonal number was quantified by counting silver-positive axonal fibers in four fields in white matter from each spinal cord section and scanned using a Leica DMLB upright microscope and QI Cam digital imaging system (Q Imaging, Pleasanton, CA) to provide digital images. Quantitative analysis of axonal damage was performed using the Adobe Photoshop and the public domain program, Image J as described previously.[29]

Immunofluorescence and Confocal Laser Scanning Microscopy

Immunohistochemistry was performed on sections (4 μm) taken from hippocampi, cerebella, and lumbar spinal cords. Deparaffinized sections were pre-incubated with 10% normal goat serum, 2% bovine serum albumin, and 0.2% Triton X-100 overnight at 4°C to prevent nonspecific binding.[29] Antigen retrieval was achieved as previously reported.[30] Double staining was performed using Alexa Fluor 488-conjugated goat anti-rabbit secondary antibody (1:500 dilution; Molecular Probes, Eugene, OR) to detect the ionized calcium-binding adapter molecule-1 (Iba-1) antibody (1:500; Wako Chemicals, Richmond, VA, Wako, Japan), and Cy-3-conjugated goat anti-mouse secondary antibody (1:500 dilution; Jackson ImmunoResearch Laboratories, Inc., West Grove, PA) to detect the mouse anti-myelin basic protein (MBP) (1:1000 dilution; Sternberger Monoclonals, Lutherville, MD) and anti-CD3 (CD3-ξ, 6B10.2, 1:100 dilution; Santa Cruz Biotech. Inc., Santa Cruz, CA) monoclonal antibodies. Control stains omitted the primary antibody. Images from each spinal cord section were scanned using a Laser Scanning System (LSM 510, Carl Zeiss Canada, Burlington, ON). The quantitative analysis of Iba-1 cell counts per square millimeter and the percentage of MBP-positive area in the white matter of spinal cords were performed as previously described.[29]

Real-Time RT-PCR

Animals were euthanized at the onset (12 dpi), peak of clinical disease (17 to 22 dpi), and the chronic phase (60 dpi) of EAE. CNS tissues were dissected-out, homogenized and then lysed in TRIzol (Invitrogen Canada, Burlington, ON) according to the manufacturer's guidelines. Total cellular RNA was isolated, dissolved in diethylpyrocarbonate-treated water; 1 μg of RNA was used for the synthesis of cDNA, and then the real-time PCR reactions were performed as described previously.[29] All mouse primer sequences were previously reported.[31,32] Semiquantitative analysis was performed by monitoring in real-time the increase of fluorescence of the SYBR-green dye on a Light Cycler (Roche, Canada, Mississauga, ON). Real-time fluorescence measurements were performed and a threshold cycle value for each gene of interest was determined. All data were normalized to GAPDH mRNA expression and expressed as the relative fold-change in mRNA level.

Statistical Analyses

Statistical analyses were performed using GraphPad Prism version 4.0 (GraphPad Software, San Diego, CA) for both parametric and nonparametric comparisons; P values of less than 0.05 were considered significant.

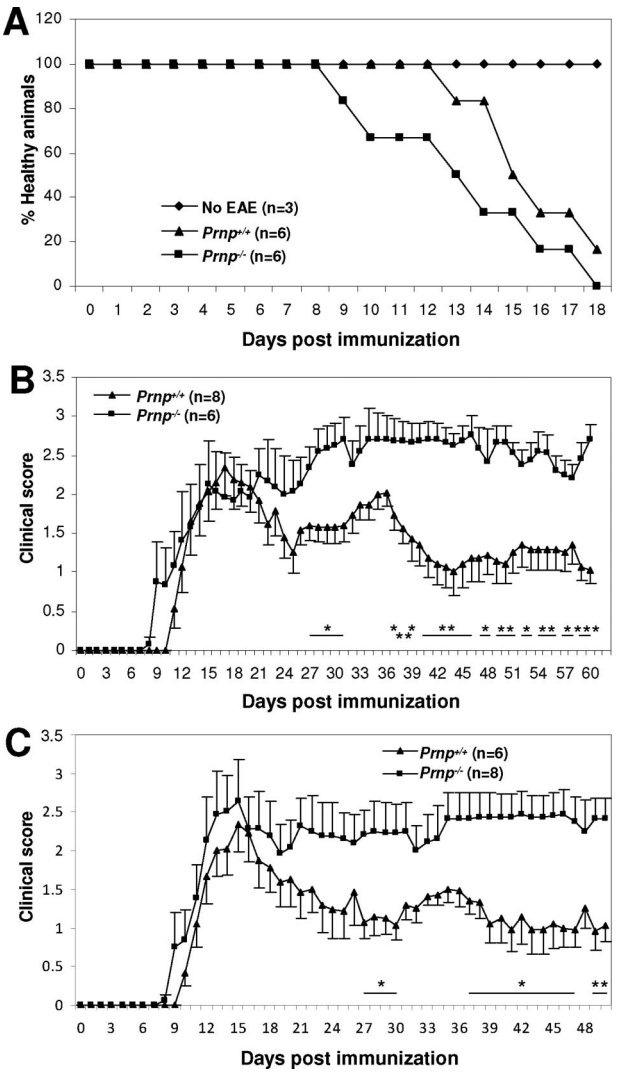

Figure 1. Neurobehavioral outcomes during EAE in $Prnp^{+/+}$ and $Prnp^{-/-}$ animals. (**A**) EAE in $Prnp^{-/-}$ animals showed an earlier onset ($Prnp^{+/+}$: 15.6 ± 0.7 vs. $Prnp^{-/-}$: 13.5 ± 1.3; 2.1 ± 0.7 days earlier, $P < 0.05$). Results are representative of two independent experiments with both experiments exhibiting the same trend. ($Prnp^{+/+}$, n = six; $Prnp^{-/-}$, n = six; No EAE control, n = three). (**B**) $Prnp^{-/-}$ animals showed higher mean clinical scores (±SEM) than wild-type littermates ($Prnp^{+/+}$). This experiment was performed independently from the early time-course experiment depicted in panel (**A**) ($Prnp^{+/+}$, n = eight; $Prnp^{-/-}$, n = six). (**C**) EAE clinical scores (±SEM) of $Prnp^{-/-}$ (n = eight) and $Prnp^{+/+}$ (n = six) mice on a C57BL/6 background. (*$P < 0.05$; **$P < 0.01$; ***$P < 0.001$; Student's t test.)

Results

PrP^C Deficiency Increases the Clinical Severity of EAE

To examine the effects of PrP^C deficiency on MOG-induced EAE, we compared disease onset and severity between $Prnp^{-/-}$ mice on a mixed genetic background and their $Prnp^{+/+}$ littermates. Relative to $Prnp^{+/+}$ mice, onset of detectable neurological dysfunction occurred earlier in $Prnp^{-/-}$ animals (2.1 ± 0.7 days earlier, $P <$ 0.05 (Figure 1A). No significant difference in clinical disease severity was observed between $Prnp^{+/+}$ and $Prnp^{-/-}$ mice starting from 12 dpi, and through the first

peak of disease and up to approximately 26 dpi (Figure 1B). *Prnp*$^{+/+}$ mice reached the peak of disease at 17 dpi, exhibited a partial remission until ~25 dpi, and this was followed by a second cycle of relapse and remission (Figure 1B). *Prnp*$^{-/-}$ mice, in contrast, not only failed to recover after the initial peak of disease, but showed increasing EAE severity, leading to sustained neurological impairment that started at approximately 28 dpi and was maintained out to 60 dpi (Figure 1B). The *Prnp*$^{+/+}$ and *Prnp*$^{-/-}$ control mice that were injected with complete Freund's adjuvant plus pertussis toxin alone, and the 'no EAE' controls that received no treatment, did not show any signs of neurological disease. To determine whether the phenotypic difference in EAE observed between *Prnp*$^{+/+}$ and *Prnp*$^{-/-}$ mixed background mice would also be observed when mice were more genetically homogenous, we induced EAE in mice that had been backcrossed onto a C57BL/6 genetic background ($N = 7$ to 8). Mice lacking the prion gene again exhibited earlier onset of EAE, and a more severe clinical disease course than littermate controls, out to 50 dpi (Figure 1C). These two sets of observations, made in mice that differed in their genetic backgrounds, demonstrated that the lack of PrP^C was associated not only with worsening of clinical EAE, but particularly with chronic neurological signs suggestive of irreversible CNS damage and/or dysfunction stemming from persistent neuroinflammation.

PrP^C Expression is Up-regulated on Activated T Cells and PrP^C Deficiency Alters the in Vitro *Responses of MOG-Primed T cells*

Generation of myelin component-reactive T cells and the subsequent infiltration of autoreactive T cells into the CNS represents a key pathogenic event in EAE.[33] The finding that PrP^C is expressed on cells of the human immune system[19,20] has suggested the possibility of a role for prion protein in the regulation of T cell responses.[34,35] However, a number of studies of PrP^C expression in the murine immune system have shown that while follicular dendritic cells, DCs, and activated lymphocytes in skin, gut- and bronchus-associated and secondary lymphoid tissues express the prion protein, most T and B cells obtained from peripheral lymphoid organs do not express detectable cell surface PrP^C.[21,22] To assess PrP^C expression on cells relevant to EAE pathogenesis, we performed flow cytometric analysis on purified populations of DCs and CD4$^+$ T lymphocytes. After gating (using the isotype control plus secondary antibody), we detected PrP^C surface expression on freshly isolated *Prnp*$^{+/+}$ DCs (Figure 2, A and B), but not on the negative control population, *Prnp*$^{-/-}$ DCs. With the anti-PrP^C antibody that we used, cell surface expression of PrP^C was undetectable on freshly-isolated resting *Prnp*$^{+/+}$ CD4$^+$ T cells. However, 48 hours after anti-CD3 antibody stimulation the majority (>80%) of CD4$^+$ cells expressed PrP^C (Figure 2, A and B). Thus, although resting naïve CD4$^+$ T cells from wild type mice failed to express detectable PrP^C, following antigen receptor-mediated activation these cells clearly express this molecule. These results

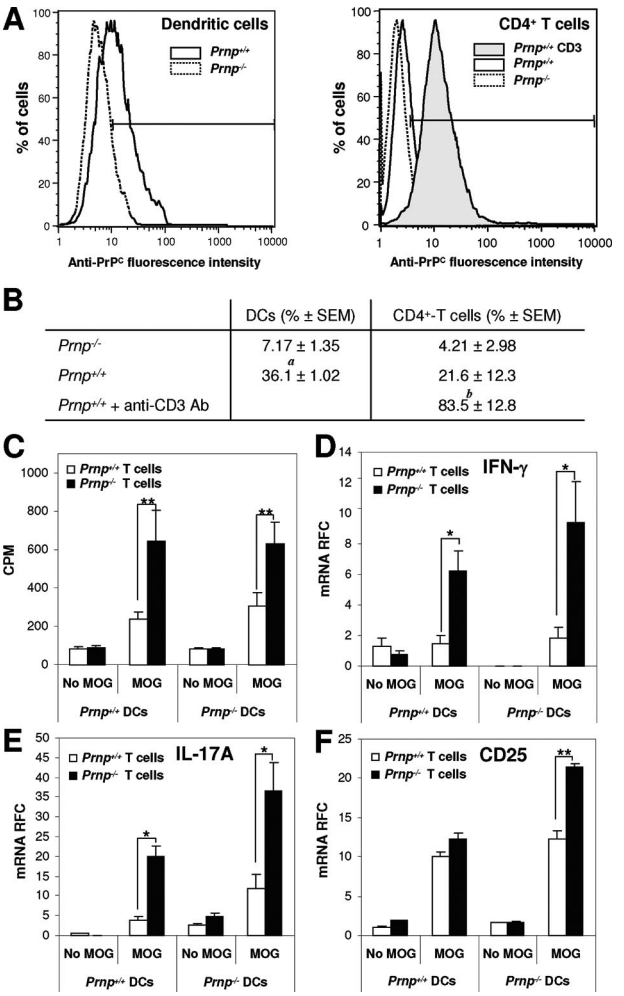

Figure 2. Cell surface PrP^C expression on DC and CD4$^+$ T cell populations, and *in vitro* studies of MOG-primed T cells from *Prnp*$^{+/+}$ and *Prnp*$^{-/-}$ animals. (**A**) Flow cytometry of *Prnp*$^{+/+}$ and *Prnp*$^{-/-}$ DCs and CD4$^+$ T cells (isolated from non-immunized animals) stained with an anti-PrP^C antibody (SAF-83). (**B**) PrP^C was expressed on *Prnp*$^{+/+}$ DCs, and although significant staining was not seen on resting *Prnp*$^{+/+}$ CD4$^+$ T cells, anti-CD3 antibody stimulation increased PrP^C expression on the majority of *Prnp*$^{+/+}$ CD4$^+$ T cells. (% ±SEM, n = four per group; $^aP < 0.0001$ vs. *Prnp*$^{-/-}$ DCs, Student's t-test; $^bP < 0.01$ vs. *Prnp*$^{-/-}$ CD4$^+$ T cells, analysis of variance, Tukey's multiple comparison test). (**C**) T cells from MOG-primed *Prnp*$^{-/-}$ mice (C57BL/6 background) showed higher proliferative responses to MOG peptide than T cells from MOG-primed *Prnp*$^{+/+}$ mice (C57BL/6 background). Total T cells isolated from lymph nodes of *in vivo* MOG-primed *Prnp*$^{+/+}$ (n = three), or *Prnp*$^{-/-}$ animals (n = three), were co-cultivated with irradiated MOG-pulsed DCs obtained from non-immunized *Prnp*$^{+/+}$ or *Prnp*$^{-/-}$ animals (C57BL/6 background). [^{3}H] thymidine incorporation was significantly higher in MOG-primed *Prnp*$^{-/-}$ T cells, regardless of the source of the DCs. Results shown are representative of two independent experiments and both experiments showed the same trend. (**D–F**) Real-time RT-PCR analysis of mean cytokine mRNA relative fold-change (±SEM) in DC-lymph node T cell co-cultures: mRNA levels for IFN-γ (**D**) and IL-17A (**E**) were significantly higher in *Prnp*$^{-/-}$ T cell cultures with either *Prnp*$^{+/+}$ or *Prnp*$^{-/-}$ DCs following MOG stimulation than in the corresponding *Prnp*$^{+/+}$ T cell cultures with either *Prnp*$^{+/+}$ or *Prnp*$^{-/-}$ DCs. IL-2Rα (CD25) mRNA expression (**F**) was up-regulated in MOG stimulated groups and *Prnp*$^{-/-}$ T cell/*Prnp*$^{-/-}$ DC co-cultures showed levels that were significantly higher than those in the *Prnp*$^{+/+}$ T cell/*Prnp*$^{-/-}$ DC co-cultures (n = five per group; $^*P < 0.05$; $^{**}P < 0.01$; Student's t-test).

are consistent with PrP^C being an activation marker in murine CD4$^+$ cells, and they demonstrate the potential for this protein to regulate some aspect of CD4$^+$ T cell activation, proliferation, or differentiation.

To functionally evaluate PrP^C-deficient lymph node T cells, CD4$^+$ T cells from MOG-primed *Prnp*$^{-/-}$ and *Prnp*$^{+/+}$ animals (C57BL/6 background) were co-cultivated with *Prnp*$^{-/-}$ or *Prnp*$^{+/+}$ MOG peptide-pulsed irradiated DCs (isolated from non-immunized mice having a C57BL/6 background) as a source of antigen-presenting cells. T lymphocyte proliferation, as assessed by [^{3}H]-thymidine incorporation, was significantly higher in the MOG-primed *Prnp*$^{-/-}$ CD4$^+$ lymph node T cells, regardless of whether these were cultivated in the presence of *Prnp*$^{+/+}$ or *Prnp*$^{-/-}$ MOG-pulsed DCs (Figure 2C). The source of the MOG-loaded DCs did not appear to have an effect on the proliferation of the MOG-primed T cells. These results suggested that immunization of *Prnp*$^{-/-}$ mice with MOG peptide led to the generation of higher numbers of MOG-reactive T cells. Although this *in vitro* assay failed to reveal a difference in *Prnp*$^{-/-}$ versus *Prnp*$^{+/+}$ DC function in terms of cell proliferation, it did not exclude the possibility of a *Prnp*$^{-/-}$-specific DC defect being exerted during the *in vivo* priming of naïve *Prnp*$^{-/-}$ T cells. Increased proliferation of *Prnp*$^{-/-}$ T cells may have accounted in part for the increased numbers of anti-CD3ε-positive cells observed in 12 dpi spinal cords of *Prnp*$^{-/-}$ mice with EAE (see Supplemental Figure S1 at *http://ajp.amjpathol.org*).

We next determined whether the increased proliferation of *Prnp*$^{-/-}$ T cells *in vitro* would be accompanied by the altered expression levels of specific cytokines. We selected two cytokines that correspond to key T cell subsets involved in EAE pathogenesis: (*i*) interferon (IFN)-γ, a product of Th1 CD4$^+$ T cells, and (*ii*) interleukin (IL)-17A, a cytokine elaborated by Th17 CD4$^+$ T cells.[36–38] Using real-time RT-PCR, we found that expression of both IFN-γ and IL-17A mRNAs were significantly up-regulated in MOG-primed *Prnp*$^{-/-}$ CD4$^+$ T cells co-cultivated with either *Prnp*$^{+/+}$ or *Prnp*$^{-/-}$ MOG-pulsed DCs (Figure 2, D and E). Interestingly, IFN-γ and IL-17A transcripts both showed a trend toward greater up-regulation when *Prnp*$^{-/-}$ CD4$^+$ T cells were cultivated with MOG-pulsed *Prnp*$^{-/-}$ DCs, however, this did not reach statistical significance. To monitor the effectiveness of MOG-induced T cell activation in the co-cultures we used expression levels of IL-2Rα (CD25) mRNA as an indicator (Figure 2F). Thus, besides showing an increase in both MOG-pulsed DC-induced proliferation and effector cytokine mRNA generation by MOG-primed *Prnp*$^{-/-}$ T cells, the results suggest that *Prnp*$^{-/-}$ DCs might have a role in regulating cytokine gene expression by T cells (Figure 2, D and E), although further studies are needed to support this notion. The increased proliferation and cytokine expression of *Prnp*$^{-/-}$ T cells in response to MOG provides a plausible explanation for disease exacerbation in the prion-deficient mice.

PrP^C Deficiency Exacerbates Spinal Cord Inflammation in MOG-Immunized Mice

Inflammatory cell infiltrates and the cytokines they produce are responsible for demyelination, alterations in neuronal function, and axonal damage in both multiple sclerosis and EAE.[39,40] Since motor dysfunction can correlate over time with spinal cord axonal pathology,[41,42] three periods were selected for analysis of the EAE spinal cords: onset (12 dpi); initial peak (17 to 22 dpi); and chronic phase (60 dpi) of disease. Within these periods, *Prnp*$^{-/-}$ and *Prnp*$^{+/+}$ mice were compared with respect to severity of inflammation, extent of demyelination, and degree of axonal loss. To gauge the extent of cellular infiltration, spinal cord sections were stained with H&E as well as an antibody specific for Iba-1, a marker for macrophages and microglia. At a time when no pathological changes were evident in *Prnp*$^{+/+}$ littermates with EAE (Figure 3A), H&E staining revealed the presence of inflammatory infiltrates in the dorsal, ventral, and lateral columns of 12 dpi *Prnp*$^{-/-}$ spinal cords (Figure 3B). Iba-1 immunoreactivity of lumbar cord sections was markedly increased, with cellular hypertrophy and infiltration in *Prnp*$^{-/-}$ animals (Figure 3F), as compared with the minimal Iba-1 immunoreactivity at 12 dpi (Figure 3E) exhibited by the controls.

At the first peak of disease (17 to 22 dpi), marked immune cell infiltration (Figure 3, C and D) and microglial activation (Figure 3, G and H) were present in both *Prnp*$^{+/+}$ and *Prnp*$^{-/-}$ mice, respectively, although quantitative analysis revealed that Iba-1-positive cells were significantly more abundant in the *Prnp*$^{-/-}$ sections (Figure 3Q). These findings were consistent with the intensity of inflammation being increased in *Prnp*$^{-/-}$ animals at the initiation of the EAE, a finding that was consistent with the earlier disease onset of *Prnp*$^{-/-}$ animals.

Since demyelination in EAE is typically related to the level of inflammation, we estimated the extent of demyelination at both disease onset and the initial peak of disease (17 to 22 dpi) by anti-MBP antibody immunofluorescence, with loss of MBP being reflective of white matter damage. Decreased MBP staining in the white matter of *Prnp*$^{-/-}$ EAE spinal cords (Figure 3, J and L) was greater than that of controls (Figure 3, I and K) both at 12 dpi and at the initial peak of disease, respectively. Of note, MBP-deficient regions contained increased densities of Iba-1-positive cells (Figure 3, O and P). Quantitative analysis of the MBP-positive spinal cord areas confirmed that MBP loss was significantly higher in *Prnp*$^{-/-}$ animals with EAE, at both 12 dpi and 17 to 22 dpi (Figure 3R), a result mirrored by the increase in Iba-1-positive cells (Figure 3Q).

In keeping with the MBP deficit observed in the dorsal cord white matter, silver staining during the chronic stage (60 dpi) of EAE revealed anatomical disruption and decreased numbers of axons in cross sections of *Prnp*$^{-/-}$ tracts (Figure 4A); this was verified by axonal counts obtained from multiple regions of the spinal cords (Figure 4, B and C). In summary, EAE in *Prnp*$^{-/-}$ mice led to a greater loss of MBP immunoreactivity in spinal cord white matter acutely, and this was accompanied in the chronic phase by an increased level of axonal drop-out, consistent with the more severe clinical disease scores seen in this phase (Figure 1, B and C).

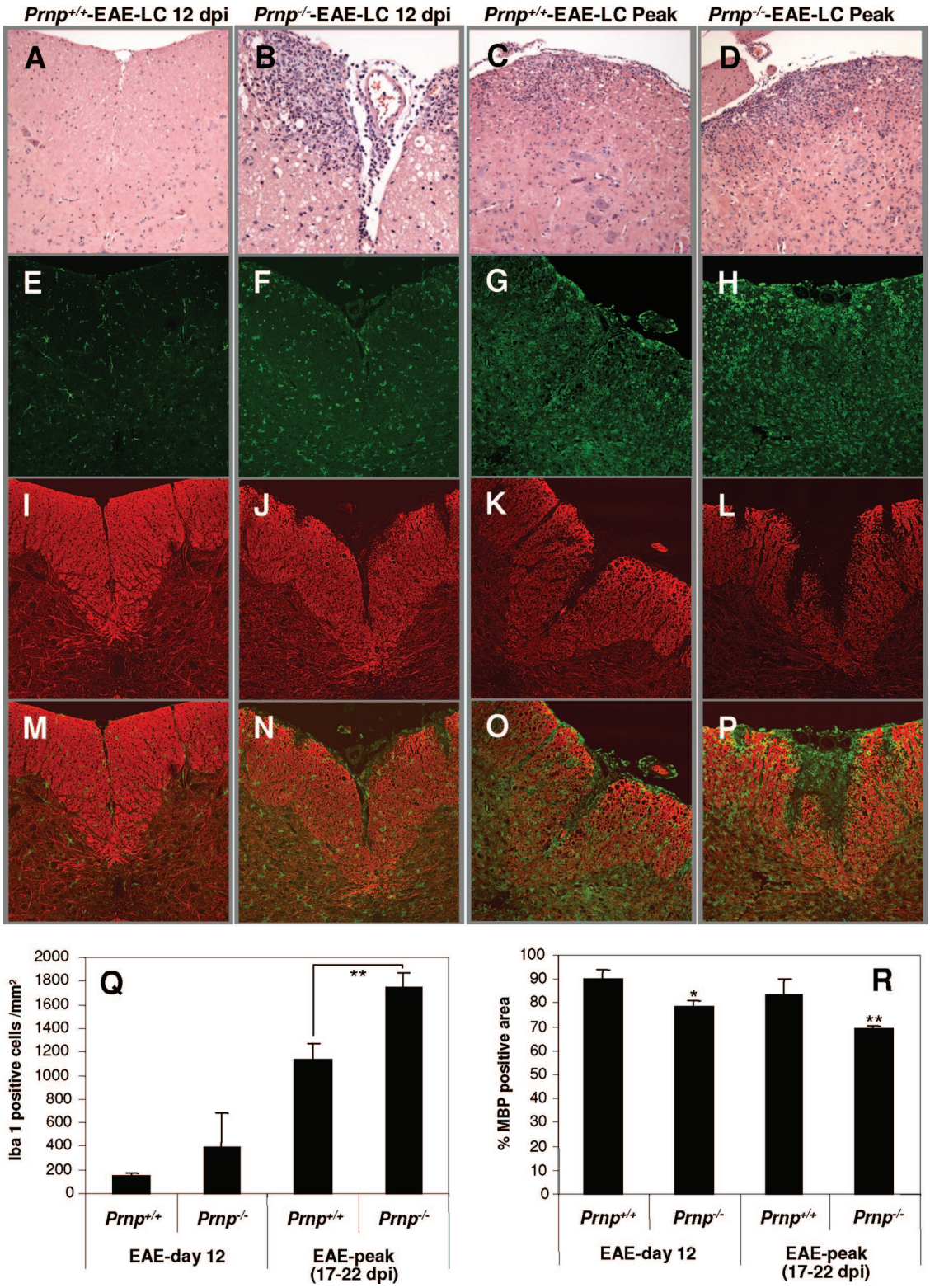

Figure 3. Neuropathological changes within representative lumbar spinal cord sections obtained from $Prnp^{+/+}$ and $Prnp^{-/-}$ animals with EAE. The columns of photomicrographs show (**A**) $Prnp^{+/+}$ lumbar cord at 12 dpi; (**B**) $Prnp^{-/-}$ lumbar cord at 12 dpi; (**C**) $Prnp^{+/+}$ lumbar cord at 17 dpi; (**D**) $Prnp^{-/-}$ lumbar cord at 17 dpi (original magnification ×200). (**E–H**) show Iba-1 immunoreactivity (green); (**I–L**) MBP immunoreactivity (red); and (**M–P**) overlay of MBP and Iba-1 immunoreactivity. (**Q**) Quantification of Iba-1^{+} immunoreactivity showed higher mean numbers of cells (±SEM) in $Prnp^{-/-}$ EAE that in $Prnp^{+/+}$ EAE. (**R**) MBP loss was determined by quantitative analysis of mean percentage of the MBP-positive area (±SEM) in $Prnp^{-/-}$ and control EAE animals from spinal cord sections taken at both 12 and 17 dpi (n = three per group, $^{*}P < 0.05$; $^{**}P < 0.01$; m, Student's t-test; n, analysis of variance, Dunnette's multiple comparison test).

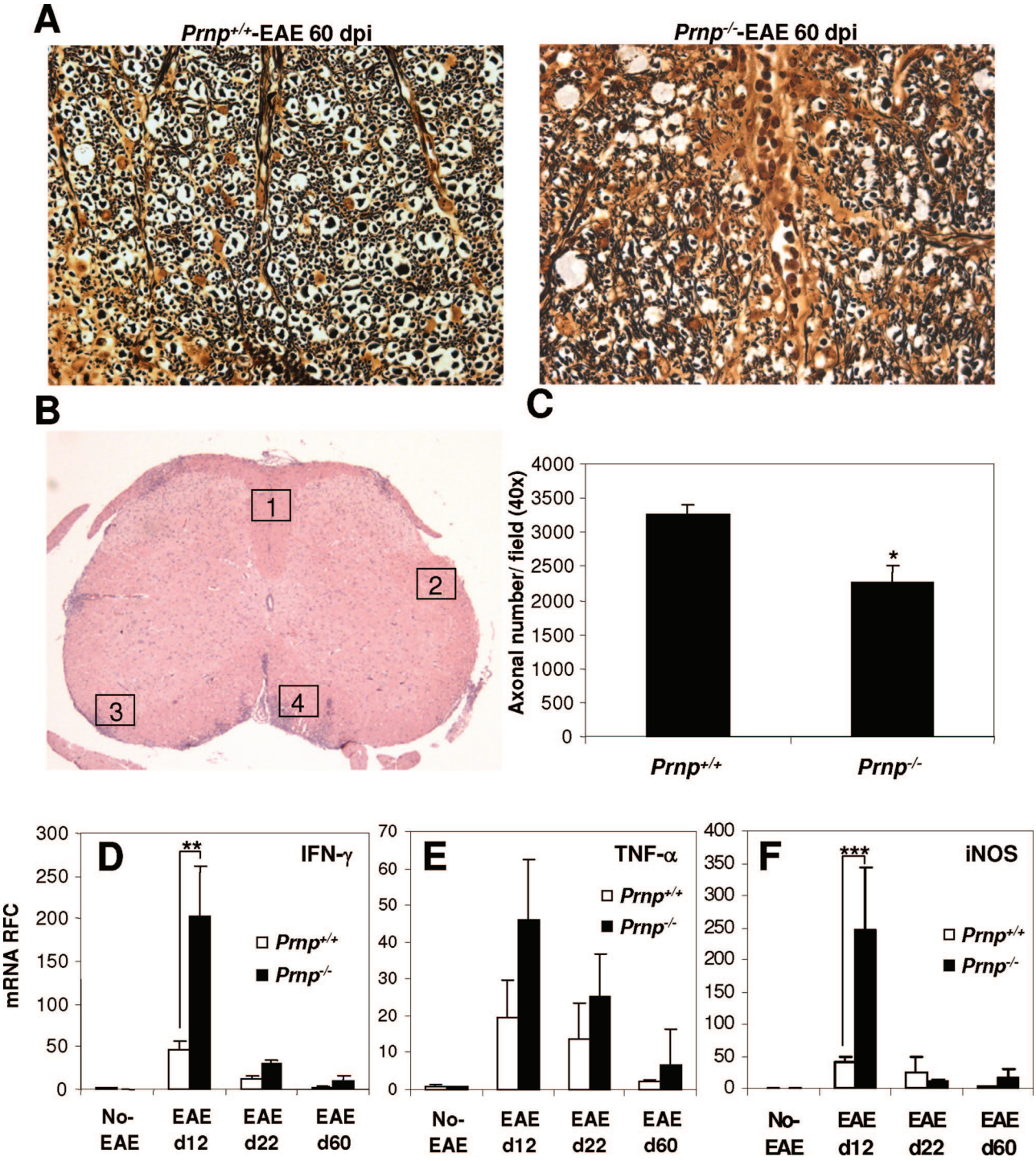

Figure 4. Spinal cord axonal damage during EAE. (**A**) Silver-stained axons within lumbar spinal cord white matter sections were less abundant in *Prnp*$^{-/-}$ than in *Prnp*$^{+/+}$ EAE (original magnification ×400). (**B**) Quantitative analysis was based on counts of silver stain-positive axons in four different areas per spinal cord section. (**C**) Mean axonal counts (±SEM) were significantly lower in *Prnp*$^{-/-}$ animals with EAE (n = five per group, $^{*}P < 0.05$, analysis of variance, Dunnette's multiple comparison test) than in controls. (**D–F**) Analyses of mean pro-inflammatory molecule mRNA relative fold-change (±SEM) in the lumbosacral spinal cord in healthy and EAE-induced *Prnp*$^{+/+}$ and *Prnp*$^{-/-}$ animals. Real-time RT-PCR showed that transcript levels for (**D**) IFN-γ, (**E**) TNF-α, and (**F**) iNOS were significantly higher in *Prnp*$^{-/-}$ EAE (filled bars) at 12 dpi compared to EAE controls when expressed as fold-increase over expression in non-EAE *Prnp*$^{+/+}$ animals (open bars). Basal mRNA levels for each gene did not differ between *Prnp*$^{-/-}$ and *Prnp*$^{+/+}$ animals. All real-time experiments were done in duplicate for each RNA sample (n = three per group, $^{*}P < 0.05$, $^{**}P < 0.01$, $^{***}P < 0.001$; analysis of variance, Tukey's multiple comparison test).

Increased Inflammatory Mediators in the Cords of PrP^C-Deficient Mice with EAE

Since PrP^C might modulate both innate and adaptive immunity by regulating the synthesis and release of cytokines and other mediators, we quantified the levels of IFN-γ, tumor necrosis factor-α (TNF-α), interleukin-1β, and inducible nitric oxide synthase (iNOS/NOS2) transcripts in EAE spinal cords by real-time RT-PCR. Consistent with the increased production of IFN-γ by MOG-primed T cells stimulated *in vitro* (Figure 2D), mRNA expression of this cytokine was significantly up-regulated within *Prnp*$^{-/-}$ lumbosacral spinal cords at 12 dpi compared to EAE controls (Figure 4D). However, expression levels did not differ between *Prnp*$^{-/-}$ and controls at the initial peak of disease (17 to 22 dpi) or during the chronic stage of EAE (60 dpi) (Figure 4D). While not reaching significance, *Prnp*$^{-/-}$ animals exhibited a trend toward increased TNF-α mRNA expression in lumbosacral cords at 12 dpi compared to *Prnp*$^{+/+}$ animals (Figure 4E); and IL-1β expression was not significantly increased in *Prnp*$^{-/-}$ lumbosacral cords (data not shown). Since nitric oxide can contribute to inflammation, oligodendrocyte injury, axonal degeneration, and neuronal death, we quantified iNOS mRNA expression in *Prnp*$^{-/-}$ and *Prnp*$^{+/+}$ EAE lumbosacral spinal cords (Figure 4F). As compared with controls, we found highly significant iNOS up-regulation in *Prnp*$^{-/-}$ samples at 12 dpi. These findings demonstrated that EAE in prion-deficient mice was accompanied by the increased generation of mRNAs encoding specific pro-inflammatory molecules, primarily IFN-γ and the macrophage/microglial cell product, iNOS/NOS2. Thus, PrP^C may play a role in regulating specific aspects of CNS inflammation.

Forebrain and Cerebellar Inflammation are Increased in PrP^C Deficient Mice with EAE

To search for forebrain and cerebellar pathology in prion-deficient mice with EAE, we performed histological and mRNA expression studies. *Prnp*$^{-/-}$ brains demonstrated striking perivascular leukocytic cell infiltrates and tissue edema that were most marked in the inner layer of *Prnp*$^{-/-}$ cerebella (Figure 5A), as well as the fimbria (Figure 6A) of 12 dpi mice. Even at the initial peak of disease (17 to 22 dpi), such infiltrates were never evident in control mice (data not shown). Figures 5A and 6A demonstrate the prominence of Iba-1-positive cells in *Prnp*$^{-/-}$ brain lesions. Consistent with the increase in inflammatory infiltrates, transcripts for IFN-γ, TNF-α, IL-1β, iNOS, and RANTES (detected by real-time RT-PCR), were more abundant in 12 dpi *Prnp*$^{-/-}$ cerebella than in the controls (Figure 5B). Only IL-17A failed to show a difference between *Prnp*$^{+/+}$ and *Prnp*$^{-/-}$ cerebella at this early stage in the neuroinflammatory disease.

Striking levels of perivascular and parenchymal infiltration by Iba-1-positive cells, and CD3-positive cells, were also observed in the chronic stage (60 dpi) of EAE in *Prnp*$^{-/-}$ brains (Figure 6B and Figure 7A) as compared with *Prnp*$^{+/+}$ EAE brains. These lesions were accompanied by increased IFN-γ mRNA expression (Figure 7B), as well as a trend toward increased levels of mRNAs encoding several pro-inflammatory molecules: TNF-α, IL-1β, iNOS, and RANTES (Figure 7B). Importantly, and unlike earlier on in the disease course (Figure 5B), IL-17A was significantly up-regulated in the cerebella of *Prnp*$^{-/-}$ of 60 dpi mice (Figure 7B). Our findings support the idea that PrP^C deficiency leads to an exacerbation and a persistence of EAE-associated neuroinflammation, possibly as a result of a heightened T cell response to MOG immunization, with pathology in the chronic phase being driven by the accumulation and/or persistence of IL-17 producing T cells.

Discussion

We have shown that PrP^C deficiency leads to an increase in the severity of EAE-related neurobehavioral and neuropathological outcomes, increased anti-MOG T cell reactivity, and a more extensive and persistent monocytic/microglial infiltration of CNS, accompanied by greater MBP loss and axonal injury. In addition to lower spinal cord involvement, striking perivascular infiltrates were observed in the white matter of the cerebella and forebrains of *Prnp*$^{-/-}$ mice, and these were also prominent during the chronic phase (60 dpi) of the disease. These pathological features were largely lacking from the control mice with EAE, suggesting that the endogenous prion gene has a suppressive effect on MOG-induced peripheral T cell responses and/or T cell-mediated neuroinflammation.

MOG peptide-induced EAE reproduces some aspects of multiple sclerosis; for example, in both diseases encephalitogenic T cells are thought to initiate neuropathology via the release of cytokines and chemokines that in turn recruit and activate macrophages and microglia.[43] The latter two cell types appear to be responsible for much of the CNS damage observed in these diseases. In the present study we found that *Prnp* deficiency was associated with earlier onset of clinical disease, and this correlated with the increased T cell infiltration and macrophage and microglial cell recruitment seen in the CNS at 12 dpi. Consistent with the more rapidly evolving pace of EAE we observed in *Prnp*$^{-/-}$ mice, T lymphocytes from these animals following *in vivo* priming demonstrated augmented proliferative responses to MOG peptide. The increased proliferation likely being reflective of a larger pool of MOG-primed T cells present in the *Prnp*$^{-/-}$ mice. Although the *in vitro* T cell proliferative response to MOG-pulsed *Prnp*$^{-/-}$ DCs was not different from that of MOG-pulsed *Prnp*$^{+/+}$ DCs, this result does not exclude the possibility that *Prnp*$^{-/-}$ DCs might exhibit a differential effect(s) during *in vivo* priming phase of the MOG peptide-reactive T cells. In summary, the greater MOG-peptide-stimulated *in vitro* responses of *Prnp*$^{-/-}$ T cells provided a plausible explanation for the earlier disease onset we observed in the CNS of *Prnp*$^{-/-}$ animals.

Assuming that the atypical EAE we observed in *Prnp*$^{-/-}$ mice was primarily attributable to a T cell defect, how might loss of this molecule alter T cell function? The

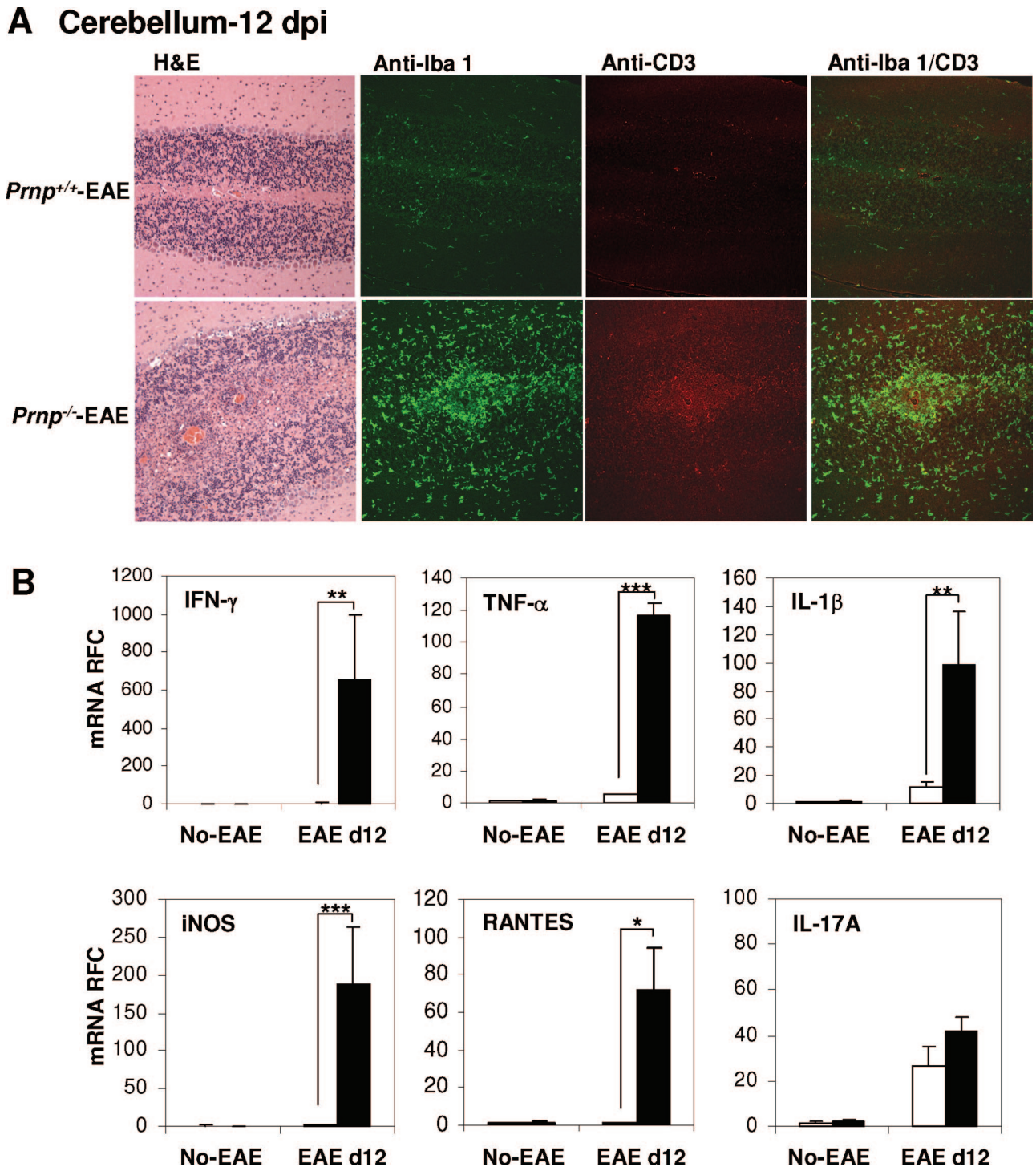

Figure 5. Representative examples of cerebellar neuropathology during the initial stages of EAE in $Prnp^{+/+}$ and $Prnp^{-/-}$ animals. (**A**) Marked perivascular infiltration was observed at 12 dpi only in $Prnp^{-/-}$ animals. Infiltrating cells were mostly Iba-1 positive and were more abundant than CD3ε-positive cells in both $Prnp^{+/+}$ and $Prnp^{-/-}$ animals at 12 dpi. (**B**) Analysis of mean pro-inflammatory molecule mRNA relative fold-change (±SEM) in lumbar spinal cords of healthy and EAE $Prnp^{+/+}$ (open bars) and $Prnp^{-/-}$ (filled bars) animals. Real-time RT-PCR showed that mRNA levels for IFN-γ, TNF-α, IL-1β, iNOS, and RANTES were significantly higher in $Prnp^{-/-}$ EAE at 12 dpi relative to $Prnp^{+/+}$ EAE, when expressed as fold-increase above expression seen in healthy $Prnp^{+/+}$ animals. IL-17A did not show significant difference between $Prnp^{+/+}$ and $Prnp^{-/-}$ EAE at this time point. Basal mRNA levels for each gene did not differ between $Prnp^{-/-}$ and $Prnp^{+/+}$ animals. All real-time experiments were done in duplicate for each RNA sample (n = three per group, $^{*}P < 0.05$; $^{**}P < 0.01$, $^{***}P < 0.001$; ANOVA, Tukey's multiple comparison test).

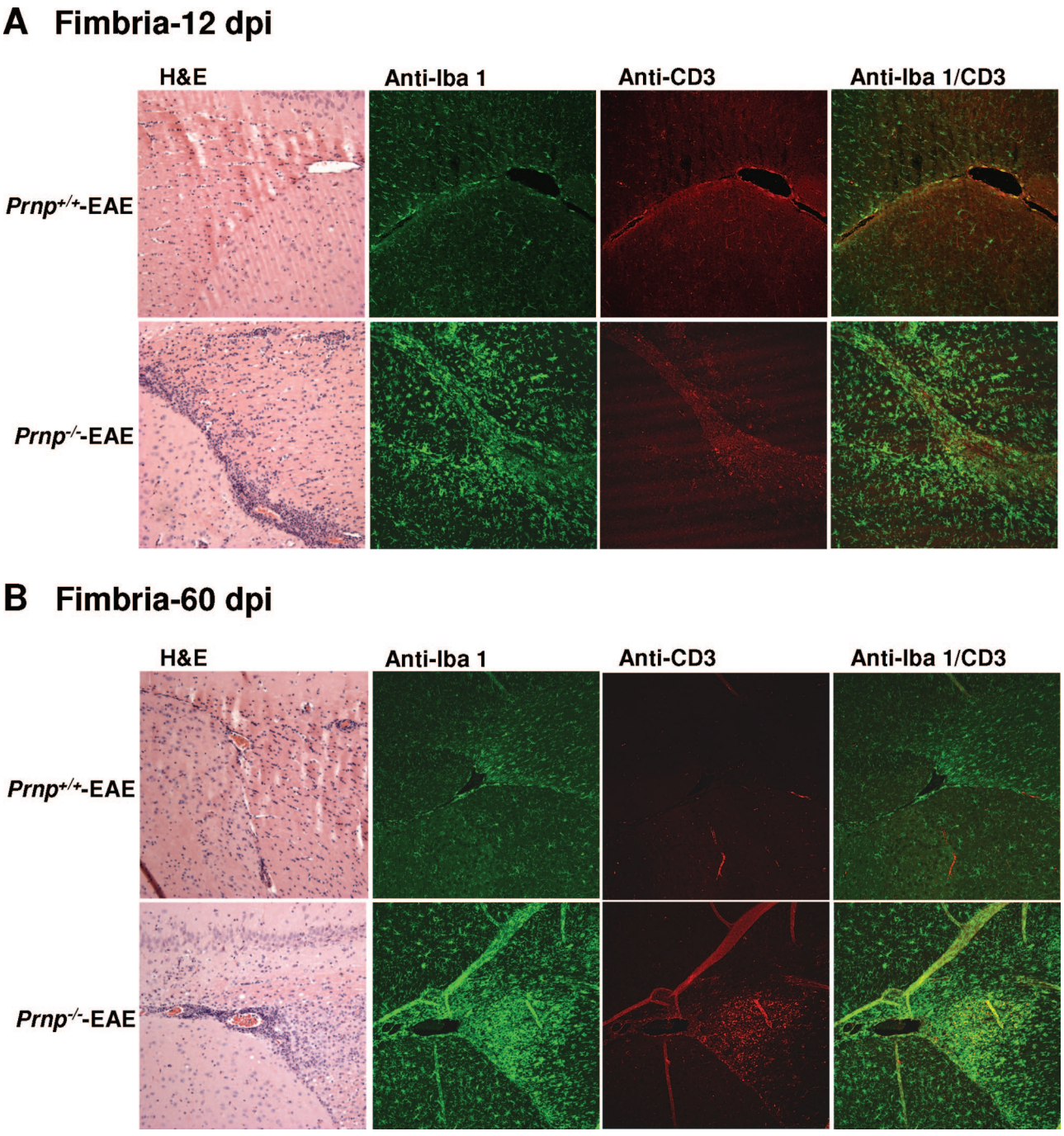

Figure 6. Representative neuroinflammatory changes in the fimbria at both the early (12 dpi) and the chronic stage of EAE (60 dpi) in $Prnp^{+/+}$ and $Prnp^{-/-}$ animals. (**A**) Only $Prnp^{-/-}$ animals showed marked perivascular and parenchymal infiltration at 12 dpi. Infiltrating cells included Iba-1^{+} cells (green), which were more abundant than CD3ε^{+} cells (red) in both the $Prnp^{+/+}$ and $Prnp^{-/-}$ mice at 12 dpi. (**B**) Iba-1 and CD3 immunoreactivity in $Prnp^{-/-}$ EAE fimbria as compared to $Prnp^{+/+}$ EAE at 60 dpi (original magnification ×200).

prion gene has been linked to various intracellular signaling pathways[44] and as with other types of glycosylphosphatidylinositol-linked glycoproteins and signal transduction complexes, PrP^{C} has been shown to be present in lipid rafts.[1] There is also evidence that the molecule has cytoprotective activity against a variety of insults,[44] although antibody-mediated cross-linking of PrP^{C}, or treatment of PrP^{C}-positive cells with the toxic fragment (PrP105-126) led to neurotoxicity.[44] Thus, if T cell PrP^{C} engagement by a ligand were to similarly deliver a pro-apoptotic stimulus to T cells, then lack of PrP^{C} would plausibly increase survival of T cells, perhaps accounting for the increased MOG-specific proliferative responses of $Prnp^{-/-}$ T cells (Figure 2C). Much still remains to be learned about the nature of the signaling pathways that are regulated by the prion molecule in T cells,[17,45–47] and how their alteration in $Prnp^{-/-}$ mice might lead to the EAE phenotype we observed.

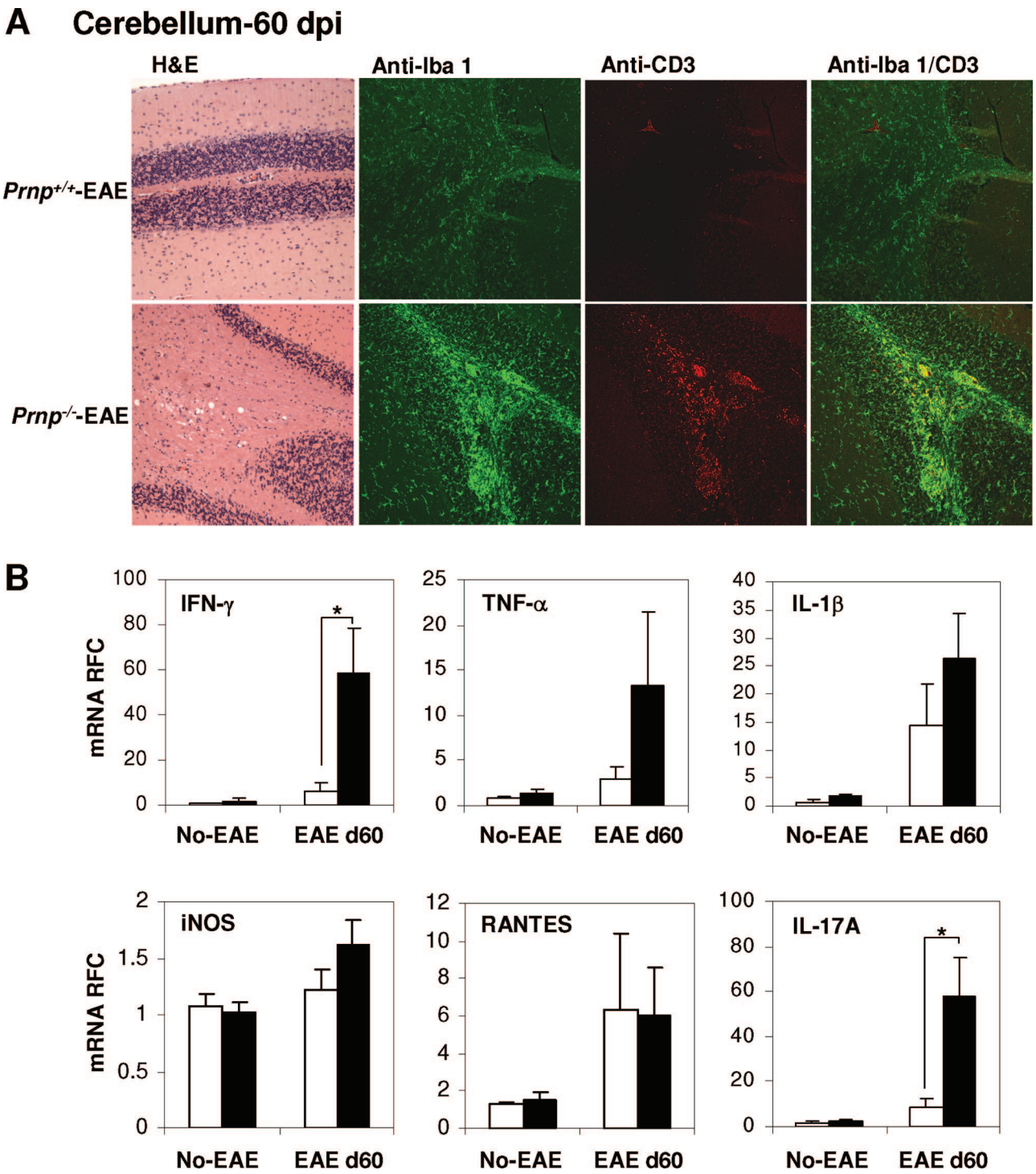

Figure 7. Neuroinflammation in *Prnp*$^{+/+}$ and *Prnp*$^{-/-}$ cerebella of mice in the chronic phase of EAE (60 dpi). (**A**) Intense Iba-1 immunoreactivity (green) was evident in *Prnp*$^{-/-}$ EAE animals at 60 dpi with CD3ε-positive cells (red) being present as compared to *Prnp*$^{+/+}$ EAE (original magnification ×200). (**B**) Analyses of mean pro-inflammatory cytokine mRNA relative fold-change (±SEM) within lumbar spinal cord samples from healthy as well as *Prnp*$^{+/+}$ (open bars) and *Prnp*$^{-/-}$ (closed bars) animals with EAE. Real-time RT-PCR showed that transcript levels for IFN-γ and IL-17A were significantly higher in *Prnp*$^{-/-}$ EAE animals at 60 dpi relative to controls with EAE. Basal mRNA levels for each gene did not differ between *Prnp*$^{-/-}$ and *Prnp*$^{+/+}$ animals. All real-time experiments were done in duplicate for each RNA sample (*Prnp*$^{+/+}$, n = eight; *Prnp*$^{-/-}$, n = six, $^{*}P < 0.01$; analysis of variance, Tukey's multiple comparison test).

PrP^{C} is up-regulated during T cell activation in humans, and we demonstrated that murine T cells also demonstrated PrP^{C} expression in response to T cell receptor-mediated cell activation (Figure 2, A and B).[48] PrP^{C} has been shown to be present within the T cell-DC 'immunological synapse',[46] and in keeping with this localization, there is some evidence of alterations in either DC function and/or T cell responses to mitogenic stimuli in *Prnp*$^{-/-}$ cells.[17] In contrast to our results, loss of prion protein was associated with either no change, or rela-

tively modest decreases, in the *in vitro* proliferative responses of T cells to stimuli, including mitogens and the mixed lymphocyte reaction.[17,25] To our knowledge, however, the consequences of prion deficiency on T cell-dependent immune responses *in vivo* have not been reported, nor has there been a study examining the potential regulatory role of PrP^C on the antigen-specific recall responses of *in vivo* primed T cells (i.e., memory cell responses). In this context, and unlike a previous study using the allogeneic mixed lymphocyte reaction to show that prion-deficient antigen-presenting cell function was reduced,[25] we found $Prnp^{-/-}$ MOG-pulsed DCs were equivalent to wild-type DCs in their ability to induce T cell proliferation and even superior in terms of their ability to elicit IFN-γ and IL-17A transcripts from these cells (Figure 2, C–E).

In view of the increased expression of IFN-γ, TNF-α, and IL-1β, it was not surprising that iNOS transcripts were greatly increased in the 12 dpi cerebella (Figure 5B), given that such cytokines activate expression of the *NOS2* gene.[49] *NOS2* expression, and hence nitric oxide generation, is known to induce inflammation, as well as oligodendrocyte and neuronal cell damage in EAE.[50] Lastly, given that PrP^C deficiency has been reported to increase cellular susceptibility to oxidative stress-induced damage,[11–13] some portion of the CNS damage that we observed in $Prnp^{-/-}$ EAE animals was potentially attributable to ROS generated by the abundant macrophages and microglia present in the EAE lesions of $Prnp^{-/-}$ mice. The elevated levels of IFN-γ in the MOG-peptide activated T cells and the CNS samples from 12 dpi $Prnp^{-/-}$ animals were in keeping with the importance of $CD4^+$ Th1 cells during the initial phase of EAE, where this cytokine appears to have an important role in endothelial cell activation, as well as in the priming of microglia and macrophages.[43,51]

Increased levels of IL-17A transcripts were particularly evident in the chronic phase of the disease in the $Prnp^{-/-}$ cerebella (Figure 7B), as were IFN-γ transcripts. Whether the two cytokines were being elaborated by the same cell type,[52] or by distinct infiltrating $CD4^+$ populations of Th1 and Th17 cells was not determined. Within the EAE lesions, IFN-γ may act to attenuate immunopathology resulting from the effects of IL-17A, in addition to its role in facilitating lymphocyte extravasation via its effects on the endothelium.[51] With respect to IL-17 in the chronic EAE lesions of $Prnp^{-/-}$ mice, it is interesting that expression-microarray analysis of multiple sclerosis samples identified IL-17 as a gene that was up-regulated in chronic lesions in humans.[53] Precisely how loss of the prion gene leads to the sustained leukocytic accumulations observed in the 60 dpi mice will require further investigation. However, if loss of PrP^C were to reduce TCR activation thresholds of anti-MOG T cell memory populations, tend to skew T cell polarization toward the Th17 phenotype, or promote the longevity of effector T cell populations (via an anti-apoptotic effect), then chronic neuroinflammation would be the predicted outcome.

Ascending progressive spinal paralysis is typical of most inbred mouse strains with EAE; however, there have been reports of atypical disease with mice showing axial rotatory locomotion and/or forelimb paralysis, in the absence of hind limb involvement, in conjunction with lesions of forebrain, cerebellum, and/or brainstem.[54] Along with the increased chronicity and CNS damage of the $Prnp^{-/-}$ EAE lesions, and in keeping with an atypical pattern of EAE, there was a striking difference in the extent of the forebrain and cerebellar inflammation in $Prnp^{-/-}$ mice as compared with controls. Clearly, prion gene deficiency was associated with a more aggressive disease phenotype, and also with a shift in the pattern of EAE to a disease that was relatively more concentrated on upper CNS structures. EAE in prion-deficient mice thus represents a novel model of neuroinflammation, with the striking lesions in the chronic phase in particular offering an opportunity for elucidating novel pathogenic mechanisms that may underlie chronicity. Our findings also raise the possibility that human prion gene polymorphisms might impact the clinical course of multiple sclerosis. Lastly, it will be of interest to determine whether the lack of PrP^C also modulates other types of adaptive immune responses, such those directed at clearing microbial infections.

Acknowledgments

We are grateful to Dr. Wee Yong for his critical review of the manuscript and many useful discussions. We also thank M. Villemaire, C. Downey, and C. Horton for maintaining the animal colony and for genotyping the mice.

References

1. Taylor DR, Hooper NM: The prion protein and lipid rafts. Mol Membr Biol 2006, 23:89–99
2. Kretzschmar HA, Prusiner SB, Stowring LE, DeArmond SJ: Scrapie prion proteins are synthesized in neurons. Am J Pathol 1986, 122:1–5
3. Brown DR, Besinger A, Herms JW, Kretzschmar HA: Microglial expression of the prion protein. Neuroreport 1998, 9:1425–1429
4. Pan T, Wong BS, Liu T, Li R, Petersen RB, Sy MS: Cell-surface prion protein interacts with glycosaminoglycans. Biochem J 2002, 368:81–90
5. Graner E, Mercadante AF, Zanata SM, Forlenza OV, Cabral AL, Veiga SS, Juliano MA, Roesler R, Walz R, Minetti A, Izquierdo I, Martins VR, Brentani RR: Cellular prion protein binds laminin and mediates neuritogenesis. Brain Res Mol Brain Res 2000, 76:85–92
6. Schmitt-Ulms G, Legname G, Baldwin MA, Ball HL, Bradon N, Bosque PJ, Crossin KL, Edelman GM, DeArmond SJ, Cohen FE, Prusiner SB: Binding of neural cell adhesion molecules (N-CAMs) to the cellular prion protein. J Mol Biol 2001, 314:1209–1225
7. Spielhaupter C, Schatzl HM: PrPC directly interacts with proteins involved in signaling pathways. J Biol Chem 2001, 276:44604–44612
8. Zanata SM, Lopes MH, Mercadante AF, Hajj GN, Chiarini LB, Nomizo R, Freitas AR, Cabral AL, Lee KS, Juliano MA, de Oliveira E, Jachieri SG, Burlingame A, Huang L, Linden R, Brentani RR, Martins VR: Stress-inducible protein 1 is a cell surface ligand for cellular prion that triggers neuroprotection. EMBO J 2002, 21:3307–3316
9. Kurschner C, Morgan JI: Analysis of interaction sites in homo- and heteromeric complexes containing Bcl-2 family members and the cellular prion protein. Brain Res Mol Brain Res 1996, 37:249–258
10. Kuwahara C, Takeuchi AM, Nishimura T, Haraguchi K, Kubosaki A, Matsumoto Y, Saeki K, Matsumoto Y, Yokoyama T, Itohara S, Onodera T: Prions prevent neuronal cell-line death. Nature 1999, 400:225–226
11. Brown DR, Nicholas RS, Canevari L: Lack of prion protein expression results in a neuronal phenotype sensitive to stress. J Neurosci Res 2002, 67:211–224

12. Wong BS, Liu T, Li R, Pan T, Petersen RB, Smith MA, Gambetti P, Perry G, Manson JC, Brown DR, Sy MS: Increased levels of oxidative stress markers detected in the brains of mice devoid of prion protein. J Neurochem 2001, 76:565–572
13. Rachidi W, Vilette D, Guiraud P, Arlotto M, Riondel J, Laude H, Lehmann S, Favier A: Expression of prion protein increases cellular copper binding and antioxidant enzyme activities but not copper delivery. J Biol Chem 2003, 278:9064–9072
14. Walz R, Amaral OB, Rockenbach IC, Roesler R, Izquierdo I, Cavalheiro EA, Martins VR, Brentani RR: Increased sensitivity to seizures in mice lacking cellular prion protein. Epilepsia 1999, 40:1679–1682
15. Weise J, Sandau R, Schwarting S, Crome O, Wrede A, Schulz-Schaeffer W, Zerr I, Bahr M: Deletion of cellular prion protein results in reduced Akt activation, enhanced postischemic caspase-3 activation, and exacerbation of ischemic brain injury. Stroke 2006, 37:1296–1300
16. Shyu WC, Lin SZ, Chiang MF, Ding DC, Li KW, Chen SF, Yang HI, Li H: Overexpression of PrPC by adenovirus-mediated gene targeting reduces ischemic injury in a stroke rat model. J Neurosci 2005, 25:8967–8977
17. Isaacs JD, Jackson GS, Altmann DM: The role of the cellular prion protein in the immune system. Clin Exp Immunol 2006, 146:1–8
18. Dodelet VC, Cashman NR: Prion protein expression in human leukocyte differentiation. Blood 1998, 91:1556–1561
19. Burthem J, Urban B, Pain A, Roberts DJ: The normal cellular prion protein is strongly expressed by myeloid dendritic cells. Blood 2001, 98:3733–3738
20. Li R, Liu D, Zanusso G, Liu T, Fayen JD, Huang JH, Petersen RB, Gambetti P, Sy MS: The expression and potential function of cellular prion protein in human lymphocytes. Cell Immunol 2001, 207:49–58
21. Liu T, Li R, Wong BS, Liu D, Pan T, Petersen RB, Gambetti P, Sy MS: Normal cellular prion protein is preferentially expressed on subpopulations of murine hemopoietic cells. J Immunol 2001, 166:3733–3742
22. Ford MJ, Burton LJ, Morris RJ, Hall SM: Selective expression of prion protein in peripheral tissues of the adult mouse. Neuroscience 2002, 113:177–192
23. Mabbott NA, Brown KL, Manson J, Bruce ME: T-lymphocyte activation and the cellular form of the prion protein. Immunology 1997, 92:161–165
24. de Almeida CJ, Chiarini LB, da Silva JP, PM ES, Martins MA, Linden R: The cellular prion protein modulates phagocytosis and inflammatory response. J Leukoc Biol 2005, 77:238–246
25. Ballerini C, Gourdain P, Bachy V, Blanchard N, Levavasseur E, Gregoire S, Fontes P, Aucouturier P, Hivroz C, Carnaud C: Functional implication of cellular prion protein in antigen-driven interactions between T cells and dendritic cells. J Immunol 2006, 176:7254–7262
26. Bueler H, Fischer M, Lang Y, Bluethmann H, Lipp HP, DeArmond SJ, Prusiner SB, Aguet M, Weissmann C: Normal development and behaviour of mice lacking the neuronal cell-surface PrP protein. Nature 1992, 356:577–582
27. Brundula V, Rewcastle NB, Metz LM, Bernard CC, Yong VW: Targeting leukocyte MMPs and transmigration: minocycline as a potential therapy for multiple sclerosis. Brain 2002, 125:1297–1308
28. Liu J, Marino MW, Wong G, Grail D, Dunn A, Bettadapura J, Slavin AJ, Old L, Bernard CC: TNF is a potent anti-inflammatory cytokine in autoimmune-mediated demyelination. Nat Med 1998, 4:78–83
29. Tsutsui S, Schnermann J, Noorbakhsh F, Henry S, Yong VW, Winston BW, Warren K, Power C: A1 adenosine receptor up-regulation and activation attenuates neuroinflammation and demyelination in a model of multiple sclerosis. J Neurosci 2004, 24:1521–1529
30. Johnston JB, Silva C, Gonzalez G, Holden J, Warren KG, Metz LM, Power C: Diminished adenosine A1 receptor expression on macrophages in brain and blood of patients with multiple sclerosis. Ann Neurol 2001, 49:650–658
31. Overbergh L, Valckx D, Waer M, Mathieu C: Quantification of murine cytokine mRNAs using real time quantitative reverse transcriptase PCR. Cytokine 1999, 11:305–312
32. Martin-Saavedra FM, Flores N, Dorado B, Eguiluz C, Bravo B, Garcia-Merino A, Ballester S: Beta-interferon unbalances the peripheral T cell proinflammatory response in experimental autoimmune encephalomyelitis. Mol Immunol 2007, 44:3597–3607
33. Hemmer B, Archelos JJ, Hartung HP: New concepts in the immunopathogenesis of multiple sclerosis. Nat Rev Neurosci 2002, 3:291-301
34. Kubosaki A, Nishimura-Nasu Y, Nishimura T, Yusa S, Sakudo A, Saeki K, Matsumoto Y, Itohara S, Onodera T: Expression of normal cellular prion protein (PrP(c)) on T lymphocytes and the effect of copper ion: analysis by wild-type and prion protein gene-deficient mice. Biochem Biophys Res Commun 2003, 307:810–813
35. Bainbridge J, Walker KB: The normal cellular form of prion protein modulates T cell responses. Immunol Lett 2005, 96:147–150
36. Komiyama Y, Nakae S, Matsuki T, Nambu A, Ishigame H, Kakuta S, Sudo K, Iwakura Y: IL-17 plays an important role in the development of experimental autoimmune encephalomyelitis. J Immunol 2006, 177:566–573
37. Langrish CL, Chen Y, Blumenschein WM, Mattson J, Basham B, Sedgwick JD, McClanahan T, Kastelein RA, Cua DJ: IL-23 drives a pathogenic T cell population that induces autoimmune inflammation. J Exp Med 2005, 201:233–240
38. Park H, Li Z, Yang XO, Chang SH, Nurieva R, Wang YH, Wang Y, Hood L, Zhu Z, Tian Q, Dong C: A distinct lineage of CD4 T cells regulates tissue inflammation by producing interleukin 17. Nat Immunol 2005, 6:1133–1141
39. Trapp BD, Peterson J, Ransohoff RM, Rudick R, Mork S, Bo L: Axonal transection in the lesions of multiple sclerosis. N Engl J Med 1998, 338:278–285
40. Tsutsui S, Noorbakhsh F, Sullivan A, Henderson AJ, Warren K, Toney-Earley K, Waltz SE, Power C: RON-regulated innate immunity is protective in an animal model of multiple sclerosis. Ann Neurol 2005, 57:883–895
41. Bjartmar C, Kidd G, Mork S, Rudick R, Trapp BD: Neurological disability correlates with spinal cord axonal loss and reduced N-acetyl aspartate in chronic multiple sclerosis patients. Ann Neurol 2000, 48:893–901
42. Wujek JR, Bjartmar C, Richer E, Ransohoff RM, Yu M, Tuohy VK, Trapp BD: Axon loss in the spinal cord determines permanent neurological disability in an animal model of multiple sclerosis. J Neuropathol Exp Neurol 2002, 61:23–32
43. Bar-Or A, Oliveira EM, Anderson DE, Hafler DA: Molecular pathogenesis of multiple sclerosis. J Neuroimmunol 1999, 100:252–259
44. Westergard L, Christensen HM, Harris DA: The cellular prion protein (PrP(C)): its physiological function and role in disease. Biochim Biophys Acta 2007, 1772:629–644
45. Mattei V, Garofalo T, Misasi R, Circella A, Manganelli V, Lucania G, Pavan A, Sorice M: Prion protein is a component of the multimolecular signaling complex involved in T cell activation. FEBS Lett 2004, 560:14–18
46. Paar C, Wurm S, Pfarr W, Sonnleitner A, Wechselberger C: Prion protein resides in membrane microclusters of the immunological synapse during lymphocyte activation. Eur J Cell Biol 2007, 86:253–264
47. Stuermer CA, Langhorst MF, Wiechers MF, Legler DF, Von Hanwehr SH, Guse AH, Plattner H: PrPc capping in T cells promotes its association with the lipid raft proteins reggie-1 and reggie-2 and leads to signal transduction. FASEB J 2004, 18:1731–1733
48. Cashman NR, Loertscher R, Nalbantoglu J, Shaw I, Kascsak RJ, Bolton DC, Bendheim PE: Cellular isoform of the scrapie agent protein participates in lymphocyte activation. Cell 1990, 61:185–192
49. MacMicking J, Xie QW, Nathan C: Nitric oxide and macrophage function. Annu Rev Immunol 1997, 15:323–350
50. Encinas JM, Manganas L, Enikolopov G: Nitric oxide and multiple sclerosis. Curr Neurol Neurosci Rep 2005, 5:232–238
51. Steinman L: A brief history of T(H)17, the first major revision in the T(H)1/T(H)2 hypothesis of T cell-mediated tissue damage. Nat Med 2007, 13:139–145
52. Suryani S, Sutton I: An interferon-gamma-producing Th1 subset is the major source of IL-17 in experimental autoimmune encephalitis. J Neuroimmunol 2007, 183:96–103
53. Lock C, Hermans G, Pedotti R, Brendolan A, Schadt E, Garren H, Langer-Gould A, Strober S, Cannella B, Allard J, Klonowski P, Austin A, Lad N, Kaminski N, Galli SJ, Oksenberg JR, Raine CS, Heller R, Steinman L: Gene-microarray analysis of multiple sclerosis lesions yields new targets validated in autoimmune encephalomyelitis. Nat Med 2002, 8:500–508
54. Muller DM, Pender MP, Greer JM: A neuropathological analysis of experimental autoimmune encephalomyelitis with predominant brain stem and cerebellar involvement and differences between active and passive induction. Acta Neuropathol (Berl) 2000, 100:174–182